Pergamon

European Journal of Cancer Vol. 32A, No. 11, pp. 1986–1994, 1996

Printed in Great Britain
0959-8049/96 $15.00+0.00

PII: S0959-8049(96)00236-5

Original Paper

^{211}At-Methylene Blue for Targeted Radiotherapy of Disseminated Melanoma: Microscopic Analysis of Tumour Versus Normal Tissue Damage

E.M. Link,[1] A.S. Michalowski[2] and F. Rösch[3]

[1]Department of Molecular Pathology, University College London Medical School, 46 Cleveland Street, London W1P 6DB, U.K.; [2]MRC Cyclotron Unit, Hammersmith Hospital, Du Cane Road, London W12 0HS, U.K.; and [3]Institute of Nuclear Chemistry, Nuclear Research Centre, D-5170 Jülich, Germany

The present stage of our preclinical investigations of targeted radiotherapy for melanoma with 3,7-(dimethylamino)phenazathionium chloride [methylene blue (MTB)] labelled with astatine-211 (^{211}At), an α-particle emitter, concerns toxicity of the treatment, as well as macro- and microscopic evaluation of its efficacy. Fragments of two human melanoma xenografts, pigmented HX118 and non-pigmented HX34 (used as a control), were implanted s.c. into nude mice subsequently treated with two doses of ^{211}At-MTB injected i.v. Alterations in tumour growth rate were related to microscopic damage caused by ^{211}At-MTB to the lesions, as determined by light microscopy using histopathological techniques. ^{211}At-MTB-dependent growth inhibition of pigmented melanoma occurred either instantly or as a gradual reduction in the tumour growth rate. At a later stage, lesions that ceased to grow immediately consisted of quiescent, heavily pigmented tumour cells, as well as advanced fibrosis, and were extensively infiltrated by melanin-laden phagocytes. Large, unresorbed and often calcified necrotic deposits characterised the tumours responding gradually to the treatment. ^{211}At-MTB remained non-toxic in normal organs. Only a relative number of small lymphocytes in the groin lymph nodes in a minority of animals was temporarily reduced, most often in conjunction with the treatment of pigmented tumours. The data demonstrated a high therapeutic effectiveness of ^{211}At-MTB towards pigmented melanoma at the expense of negligible injury to normal tissues, and revealed that the macroscopic determination of tumour growth rate often underestimated an efficacy of the applied treatment.

Key words: melanoma, targeted radiotherapy, radiolabelled methylene blue, astatine-211, α-particles, radiation damage

Eur J Cancer, Vol. 32A, No. 11, pp. 1986–1994, 1996

INTRODUCTION

EARLY DISSEMINATION of cutaneous melanoma to distant unpredictable locations makes treatment of this neoplasm exceptionally difficult [1]. As the invading melanoma tends to spread through both the lymphatic and the blood vessels, only a systemic treatment that reaches all tumour cells, irrespective of whether singly dispersed and in circulation or already forming solid tumour deposits, might prove curative.

Correspondence to E.M. Link.
Received 21 Dec. 1995; revised 26 Mar. 1996; accepted 7 Jun. 1996.

Targeted radiotherapy with astatine-211 (^{211}At) 3,7-(dimethylamino)phenazathionium chloride 'methylene blue' (^{211}At-MTB) seems to fulfil the requirement [2]. The treatment is addressed selectively to melanoma cells because of the high affinity of MTB for melanin synthesised in the tumour cells [3]. Most melanomas are pigmented and this melanin, unlike that in normal tissues, is stably localised within the tumour, presenting a distinct target for the radioisotope carrier. Administered systemically, MTB penetrates easily into the melanoma cells and their melanosomes, forming a firm complex with melanin. Although the mechanism underlying such high affinity for MTB has not been

defined fully, a formation of charge-transfer complex [3–6] and van der Waals' forces occurring at the conjunctions of the aromatic rings of the compound and the aromatic indole nucleus of melanin [7] have been suggested to be predominantly responsible for the strong binding of MTB to this biopolymer. The capacity of melanin to form so strong a complex with MTB results in a selective uptake of the compound in tumour cells as shown *in vitro* [8, 9], as well as *in vivo* in animals and man [10, 11].

Choice of the appropriate radioisotopes, governed by their physical properties [12], is equally important in assuring the maximum efficacy of targeted radiotherapy. From a selection of three radionuclides that might be suitable for systemic treatment with MTB as a carrier, namely ^{35}S (β-emitter), ^{125}I (Auger-electron emitter) and ^{211}At (α-particle emitter), the cytocidal efficacy of ^{211}At-MTB proved to be two orders of magnitude higher than that of the other MTB radioderivatives [9].

^{211}At is produced by the ^{209}Bi(α, 2n)^{211}At nuclear reaction using an external beam of 28 MeV α-particles. ^{211}At ($T_{1/2}$ = 7.2 h) decays by two pathways, with one α-particle emitted per disintegration [13]. The mean range of α-particles emitted by ^{211}At amounts to 60–65 μm (this corresponds to 3–6 cell diameters). Their high linear energy transfer (LET) of 98.84 keV/μm unit density tissue is close to the optimum (100 keV/μm) at which an oxygen enhancement ratio (OER) of approximately 1 and maximum relative biological effectiveness (RBE) are achieved [14]. These features of α-particles from ^{211}At bound to MTB assure that most energy carried by the emitted radiation is deposited within melanoma cells and should result in a highly efficient treatment without associated damage to normal organs and tissues.

The ability of ^{211}At-MTB to scavenge blood-circulating melanoma cells and eradicate micrometastases, as well as to inhibit the growth of solid tumours, was determined for human melanoma xenografts grown in athymic mice. A single i.v. injection of ^{211}At-MTB given after i.v. inoculation of singly dispersed melanoma cells reduced the number of pulmonary tumour colonies to below 10% of controls, regardless of the time that elapsed between cell implantation and the treatment [15]. The result was of particular significance, as it applied to cells with a limited melanin content used deliberately to imitate the frequent pattern of pigmentation found in human metastatic lesions [15]. More advanced clinical stages of tumour development were mimicked by s.c. transplantation of spontaneously metastasising human melanoma xenografts into nude mice subsequently treated by one or multiple i.v. injections of ^{211}At-MTB. The treatment invariably deterred the growth of both cutaneous tumours and metastases [16, 17]. The fractionation regime of ^{211}At-MTB delivery, as well as melanin content and size of the lesions, were major determinants of the treatment efficacy that varied from transient to permanent growth inhibition of the cutaneous tumours [16, 17]. Pigmentation level in cells initiating the development of metastases was of less importance and ^{211}At-MTB controlled the spread of melanoma even from the cutaneous tumours that did not respond significantly to the treatment [16, 17].

The described data implicate a high effectiveness of ^{211}At-MTB employed as adjuvant therapy for this exceptionally malignant neoplasm. However, existing prejudice against systemic application of α-particle emitters in man, together with the pioneering character of ^{211}At-MTB treatment, called for extensive toxicological studies to demonstrate that ^{211}At bound to an appropriate carrier does not display severe toxicity towards normal structures. In the present studies, the effects of ^{211}At-MTB in normal organs were compared at the light microscopic level with damage caused to the melanoma lesions. Tumour-size dependence of response to ^{211}At-MTB treatment was also investigated microscopically.

MATERIALS AND METHODS

Human melanoma xenografts

Two human melanoma xenografts, a highly pigmented HX118 and a poorly pigmented HX34, were obtained from the Institute for Cancer Research (Sutton, Surrey, U.K., courtesy of Professor G. G. Steel). Both lines were derived from biopsy samples of secondary lymph node deposits from patients who had not undergone prior cytotoxic therapy. Xenografts were established in nude mice by J. Mills of the same Institute and their properties determined, including the response to ionising radiation described previously [18, 19]. The obtained samples contained 2 mm^3 tumour pieces frozen in 10% dimethyl sulphoxide at their fourth passage *in vivo*.

The material used in our experiments was always taken from s.c. tumours grown in nude mice and passaged every 3–4 weeks (HX34) or 5–6 weeks (HX118) by transplanting two to four tumour fragments suspended in 0.2 ml Eagle's Modified Medium (Flow Laboratories Ltd, Irvine, U.K.).

Transplantation of tumour fragments

HX118 and HX34 melanoma excised from mice were placed in Petri dishes containing Eagle's Modified Medium. The tumours were cut into small pieces (approximately 1 mm^2) and one such fragment suspended in 0.1 ml medium was implanted s.c. at the inguinal region on both sides so as to initiate growth of two tumours in each mouse.

Experimental animals

All experiments were carried out using 50–60 day-old female nude mice (Crl:nu-nu(CD/1)BR) supplied by Charles River (U.K.). The animals were kept in sterile cages covered with sterile filters and fed with sterilised food and water. The experiments were performed under sterile conditions using a laminar flow cabinet (Flow Laboratories Ltd). Intravenous injections of ^{211}At-MTB were carried out on animals anaesthetised with fluothan.

^{211}At-MTB

^{211}At production and the synthesis of ^{211}At-MTB were carried out in the Department of Radioisotopes, Central Institute for Nuclear Research (Rossendorf, Germany), using a 28 MeV α-particle external beam from the Rossendorf U-120 cyclotron. ^{211}At characterised by a purity higher than 99% was obtained (^{210}At contamination amounted to 4×10^{-6} only) [20]. An electrophilic substitution reaction was used for labelling MTB with the radioisotope. Since the half-life of ^{211}At equals 7.2 h, an aqueous solution of ^{211}At-MTB with specific activity of approximately 200 MBq/mg was made before each experiment and

diluted in phosphate-buffered saline to the desired radioactivity per unit volume. An aliquot of 0.1–0.15 ml of the final solution was injected i.v. into one of the tail veins of melanoma-bearing mice.

Microscopic analysis of tumour and normal tissue damage after treatment with ^{211}At-MTB

Toxicological studies aimed at establishing the nature and severity of tissue damage caused by α-particles emitted during ^{211}At-MTB treatment in both melanoma lesions and several organs were carried out over a period of 3.5 months. Nineteen nude mice bearing two s.c. inguinal melanomas each were treated with two fractions of ^{211}At-MTB. The first dose of 8 MBq was administered 7 days after inoculation of the tumours, the other (7.3 MBq) 21 days later. Although it was established previously [16, 17] that the optimal time interval between two sequential ^{211}At-MTB fractions to obtain maximum therapeutic gain amounted to 5–7 days, the 3 weeks used here enabled an analysis of the development of tumour damage caused by each ^{211}At-MTB dose given. ^{211}At-MTB radioactivity used per fraction was dictated by our previous calculations concerning tumoricidal doses from this astatinated compound deposited in pigmented tumours [9] and biodistribution studies [10, 11]. A single dose of 24 MBq ^{211}At-MTB injected i.v. was found to be sufficient to cause complete remission of the tumour, provided a homogeneous distribution of the compound within the lesion could be achieved (for detailed calculations see [9, 16]). As such a dose seemed too high to be administered in a single injection, it was split into smaller fractions [16, 17].

Mice selected randomly at 36 h and, subsequently, with a diminishing frequency 4–32 days after every ^{211}At-MTB injection were sacrificed under general anaesthesia by perfusion with a mixture of paraformaldehyde (2%) and glutaraldehyde (2.5%) in cacodylate buffer (0.1 M, pH 7.2) through the left heart ventricle. Tumours, heart, lungs, stomach, intestines, liver, gallbladder, kidneys, urinary bladder, spleen, lymph nodes, adrenals, thyroid and eyes were excised, fixed further with 10% formal saline and prepared for light microscopic examination following standard methods, including haematoxylin and eosin staining [21].

Additionally, ^{211}At-MTB at a total dose of 23–24.5 MBq injected as three fractions at 7 days' intervals was administered to five tumour-free mice to enable an open-ended observation of the effects of the treatment on the animals.

Eleven control mice, each bearing two inguinal tumours with their size corresponding to those subsequently exposed to ^{211}At-MTB and used for comparison, were not treated with either cold MTB or free $^{211}At^-$, as neither interfered with the growth of melanoma at the concentration/radioactivity used, as shown in our previous investigations [8, 9]. Furthermore, free $^{211}At^-$ at doses 4.5 times lower than those employed at present for ^{211}At-MTB treatment was toxic or even lethal to mice [22]. The control animals could not, therefore, be injected with high enough doses of $^{211}At^-$ and were given none.

Therapeutic effectiveness of ^{211}At-MTB—macroscopic evaluation

Macroscopic evaluation of the therapeutic efficacy of ^{211}At-MTB was carried out in parallel with the toxicity studies to determine to what extent microscopic damage is reflected by macroscopic changes in tumour size resulting from the treatment. The growth rate of treated versus control tumours served as the criterion of therapeutic effectiveness of ^{211}At-MTB. The growth rate of cutaneous melanoma implanted inguinally into nude mice was determined by calculating a ratio of tumour size at intervals after ^{211}At-MTB injection to a size of the tumour at the time of introduction of the treatment. The tumour size was calculated, as previously [8, 16, 17], from repeated calliper measurements of three diameters of the lesions: the greatest one, the perpendicular to it and the thickness. A thickness of the skin in the close proximity of the tumours was determined in every mouse and subtracted from a thickness of the lesion. The measurements were initiated before an introduction of the treatment to ensure that the precise size of every lesion would be known at the time of the first ^{211}At-MTB injection. Thirty-eight treated and 22 control tumours were evaluated. When their number diminished with time to four per experimental point, due to sacrifice of mice necessary for parallel toxicological studies, a standard deviation was not calculated further and a dashed line, rather than a continuous one, was drawn through the data points to signify the change (see Figure 1).

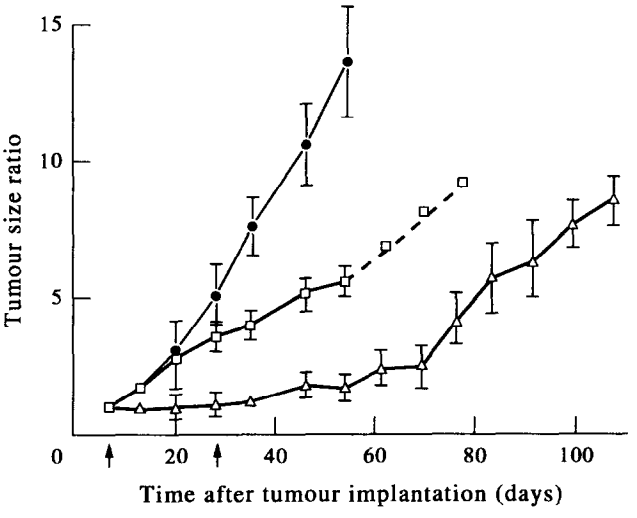

Figure 1. Two patterns of growth of pigmented HX118 human melanoma inoculated s.c. into nude mice: tumours gradually diminishing their growth rate after ^{211}At-MTB treatment (□) and lesions temporarily ceasing to grow after ^{211}At-MTB administration (△). Two fractions of ^{211}At-MTB were injected i.v. as indicated by arrows, i.e. 7 and 28 days after tumour implantation. Control, untreated tumours (•). Error bars show ± standard deviation.

RESULTS

Macroscopic changes in tumour size after ^{211}At-MTB treatment

The growth rate of untreated HX118 and HX34 melanoma xenografts was dependent only on their pigmentation, but for each type did not vary significantly ($P > 0.1$) between the subgroups, regardless of the initial size of the tumours [17].

1. *Tumour growth rate of pigmented HX118 melanoma treated with ^{211}At-MTB.* Pigmented melanoma responded to ^{211}At-MTB treatment non-uniformly (Figure 1). Tumours that were larger at the introduction of the treatment (on average 3 mm × 1.7 mm in perpendicular diameters and

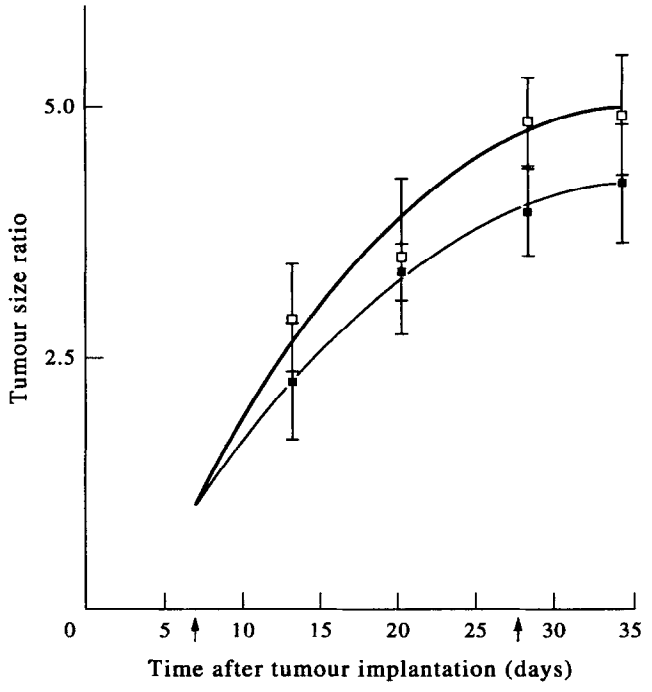

Figure 2. Growth of non-pigmented HX34 human melanoma inoculated s.c. into nude mice and treated with two fractions of ^{211}At-MTB administered i.v. as indicated by arrows, i.e. 7 and 28 days after tumour implantation (□). Control, untreated tumours (■). Error bars show ± standard deviation.

0.2 mm thick on day 7 after implantation) slowed in growth gradually with time after ^{211}At-MTB administration. A maximum reduction in their growth rate, as calculated on day 56 after their inoculation, was 63% as compared to control values. Subsequently, the tumours gradually accelerated their growth rate, but never achieved that of untreated lesions ($0.05 < P < 0.1$).

The growth of the remaining, smaller tumours (on average 2.6 mm × 0.9 mm in perpendicular diameters and 0.1 mm thick on day 7 after implantation) was inhibited instantly by the first dose of ^{211}At-MTB (Figure 1). The second ^{211}At-MTB fraction prolonged this lag phase for a further 8 days and the lesions subsequently began to grow slowly reaching 5% of the control growth rate 56 days after their inoculation. By day 107, the growth rate of these tumours increased significantly but continued to remain at a lower value than that of untreated lesions and amounted to approximately 60% of the control values ($P < 0.02$).

2. *Tumour growth rate of non-pigmented HX34 melanoma treated with ^{211}At-MTB.* ^{211}At-MTB administered to mice bearing non-pigmented melanoma did not diminish the growth rate of the tumours (Figure 2). The size of both control and treated lesions increased with time in a similar manner; therefore, there was no macroscopic evidence of any therapeutic effect from the applied ^{211}At-MTB.

Microscopic damage to melanoma tumours in ^{211}At-MTB-treated mice

1. *Pigmented HX118 melanoma xenografts.* The microscopic appearance of the untreated control tumours was typical of human melanotic melanoma growing in the natural host, with tightly arranged epithelioid cells and small foci

Figure 3. Untreated xenograft of pigmented HX118 human melanoma grown s.c. in a nude mouse. Melanin is most clearly visible in the vicinity of the subcapsular blood vessels on the left. A small area of fresh tumour necrosis occupies the mid-portion of the right margin. Haematoxylin and eosin staining, magnification ×100.

of coagulative necrosis (Figure 3). The area occupied by the necrotic tissue increased significantly with the time that elapsed from the implantation of tumour fragments into mice, but the overall design of the tumour structure remained unchanged.

In the microscopic analysis of tumours treated with ^{211}At-MTB, as they responded to treatment in two alternative manners (Figure 1), the findings are described separately for each pattern of changes in tumour size.

Tumours gradually diminishing their growth rate after ^{211}At-MTB administration. Six days after the first ^{211}At-MTB injection, these lesions presented early perivascular oedema and an extensive vacuolar degeneration of tumour cells encircling the blood vessels (Figure 4a). The damage progressed with time to widespread tumour necrosis. Such necrotic tissue surrounded nests of viable tumour cells with the blood vessel located in their centre (Figure 4b). Most of these viable cells were subsequently damaged by the second dose of ^{211}At-MTB. This resulted in the fresh coagulative necrosis of the tumour (Figure 4c). The few melanoma cells still viable after the second ^{211}At-MTB injection were attached to either a functional capillary or blood vessel occluded by thrombotic masses (Figure 4d). However, after time had elapsed following treatment, dilated blood vessels became entirely surrounded by necrotic tumour tissue (Figure 4d). The unresorbed necrotic masses tended to calcify in the form of grains (Figure 4(e)i) or microstones (Figure 4e(ii)) of calcium salt deposits. The viable tumour residue did not differ in its microscopic appearance from untreated melanoma and, as ^{211}At-MTB was not administered for the third time, these cells initiated the subsequent regrowth of the lesions. Since the dead tumour tissue had not been resorbed but mostly remained, the size of the lesions did not diminish after treatment and, consequently, grossly underestimated the effectiveness of ^{211}At-MTB therapy (Figure 1).

^{211}At-MTB-treated lesions temporarily ceasing to grow. An early reaction of these tumours occurring 6 days after the first ^{211}At-MTB dose consisted of areas of incipient necrosis with liquefaction (Figure 5a). Seven days later, foci of coa-

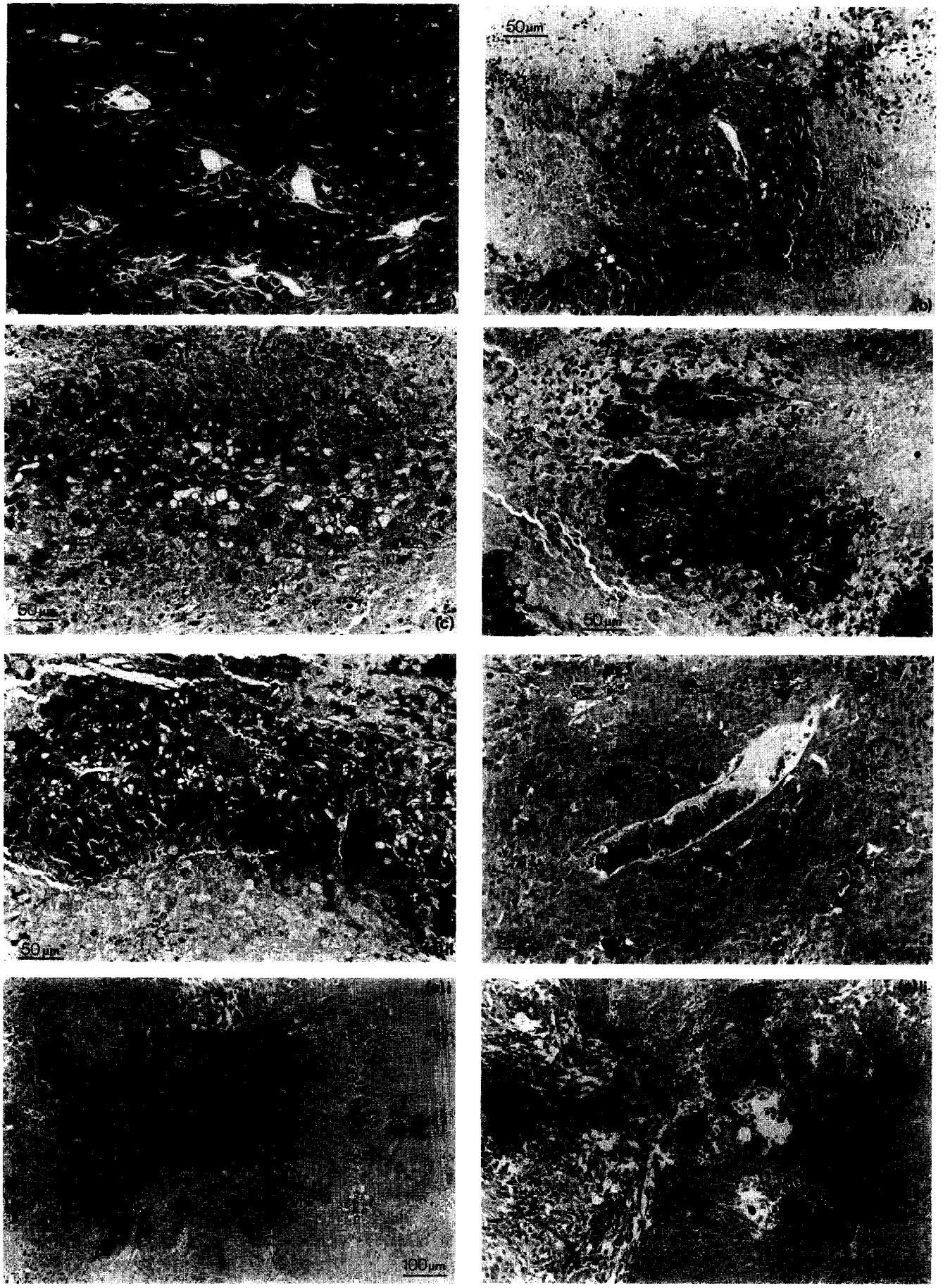

Figure 4

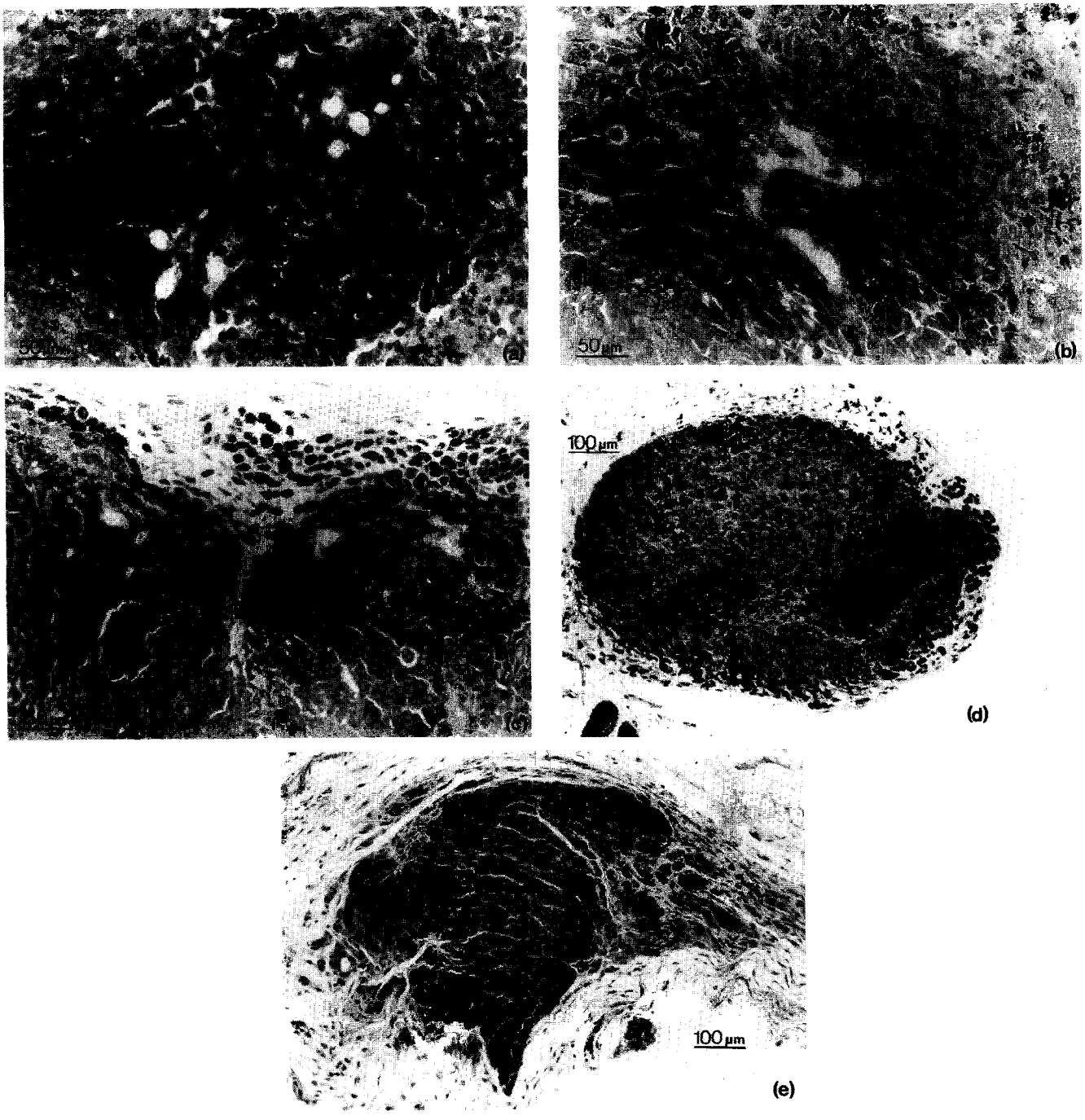

Figure 5. Microscopic appearance of pigmented HX118 human melanoma inoculated s.c. into nude mice and treated with ^{211}At-MTB as described in Figure 1, pattern of growth (△). Haematoxylin and eosin staining. (a) Early reaction of the tumour consists of areas of incipient necrosis with liquefaction (right two-thirds of the field) as observed 6 days after the first ^{211}At-MTB administration. Magnification ×200. (b,c) Abundant melanin present in the phagocytic cells accompanying the blood vessel (b, arrow) and accumulating in the tumour capsule (c) as found 13 days after the first ^{211}At-MTB injection. Magnification ×200. (d) A small focus of fresh necrosis (arrow) in a larger area in which individual tumour cells are separated by earlier deposits of collagen 2 days after the second dose of ^{211}At-MTB. A peripheral cap (on the right) consists of the so-called dormant or quiescent, heavily pigmented melanoma cells with their nuclei smaller and denser than usual. Magnification ×100. (e) Entire tumour composed of dormant cells and more advanced fibrosis. The melanin-laden phagocytes are present in the tumour bed. Magnification ×100.

Figure 4. [Opposite] Microscopic appearance of pigmented HX118 human melanoma inoculated s.c. into nude mice and treated with ^{211}At-MTB as described in Figure 1, pattern of growth (□). Haematoxylin and eosin staining. (a) Early perivascular oedema with a vacuolar degeneration of tumour cells 6 days after the first ^{211}At-MTB injection. Magnification ×200. (b) A widespread tumour necrosis surrounding a typical nest of the viable tumour with the central blood vessel as found 19 days after the first ^{211}At-MTB injection. Magnification ×200. (c) Tumour response observed 6 days after the second dose of ^{211}At-MTB: central blood vessel encircled by degenerating tumour cells with fresh peripheral coagulative necrosis. Magnification ×200. (d) Further progression of tumour damage caused by two doses of ^{211}At-MTB: (i) small groups of viable tumour cells with functional capillaries in the centre (magnification ×200); (ii) blood vessel partially occluded by thrombotic masses (magnification ×200); (iii) partly dilated blood vessel entirely surrounded by necrotic tumour tissue (magnification ×200). (e) Calcification of unresorbed necrotic tumour masses 4 weeks after completion of ^{211}At-MTB treatment: (i) calcium salt deposits as dark grains (magnification ×100); (ii) calcium salt deposits as microstones (magnification ×100).

gulative necrosis contained abundant melanin that was also present in the phagocytic cells of the host accompanying the blood vessels and accumulating in the tumour capsule (Figure 5b,c). Two days after the second dose of ^{211}At-MTB, small foci of fresh necrosis were observed in larger areas in which individual melanoma cells had been separated by earlier deposits of collagen (Figure 5d). A significant proportion of every lesion consisted of the so-called dormant or quiescent, heavily pigmented tumour cells with their nuclei smaller and denser than usual (Figure 5d). At a later stage of the damage caused by ^{211}At-MTB, almost entire lesions were composed of such cells and more advanced fibrosis (Figure 5e). The phagocytes laden with melanin were present in the tumour bed as provided by the murine host (Figure 5e).

2. *Non-pigmented HX34 melanoma xenografts.* Unlike the pigmented melanoma, xenografts of the non-pigmented variety did not show clear microscopic signs of damage caused by ^{211}At-MTB treatment. The tumours of both control mice and those subjected to the therapy consisted of viable melanoma cells with fresh focal necrosis, often haemorrhagic.

Effects of ^{211}At-MTB treatment in normal organs

^{211}At-MTB treatment affected only the thyroid, regional lymph nodes and lungs. The observed changes were minor, temporary and occurred only in some of the animals.

In the thyroid of 23% of the mice treated with ^{211}At-MTB, there was a focal interstitial oedema with scanty mononuclear infiltration, as well as moderate depletion and flattening of the epithelium of a few follicles (Figure 6). Such changes occurred predominantly 5–6 days after the second administration of ^{211}At-MTB. The structure of the gland returned to normal over the following 6 weeks (it should be pointed out that, although ^{211}At possesses a similar affinity for the thyroid as iodine, none of the thyroids were blocked with either potassium iodide or potassium perchloride prior to ^{211}At-MTB administration).

Some lymph nodes in the groin presented a segmental reduction in the number of cortical small lymphocytes (Figure 7). Although such a change was observed in only one control (HX118) and one ^{211}At-MTB-treated mouse bearing the HX34 melanoma xenograft, it affected approximately a third of treated animals with pigmented HX118 tumours. The loss of lymphocytes was first seen 5 days after the first ^{211}At-MTB administration, and their number returned to normal within the next 3 weeks.

The lungs were not affected directly by ^{211}At-MTB. Individually dispersed melanin-laden phagocytes were lodged in the alveolar walls and around the blood vessels of the organ in mice bearing pigmented melanoma and treated with ^{211}At-MTB 2–3 months earlier (Figure 8). Such cells were never observed in control animals.

Long-term observation (for up to 17 months) and subsequent microscopic examination of tumour-free mice treated with ^{211}At-MTB did not disclose any treatment-related pathology.

It should be pointed out that athymic (nude) mice do not contain melanin in normal ocular and cerebral structures, or in the skin. Thus, it was necessary to carry out additional toxicological investigations in highly pigmented C57Black mice to evaluate ^{211}At-MTB effects in melanin-laden normal tissues. These studies did not reveal any significant alterations in the eye (a detailed account of the results will be reported in a separate paper). Cerebral pigmented tissues, such as substantia nigra or locus coeruleus, on the other hand, are only present in primates. However, although it was impossible to assess toxicity of ^{211}At-MTB in such structures in mice, our biodistribution studies in man disclosed the existence of a blood–brain barrier for radiolabelled MTB [11] that prevents the compound from being taken up by normal pigmented cerebral structures, ultimately protecting them from potential ^{211}At-MTB-mediated damage. Similarly, a lack of vasculature in the epidermis precludes a blood-derived supply of ^{211}At-MTB to normal melanocytes that remain intact after the treatment.

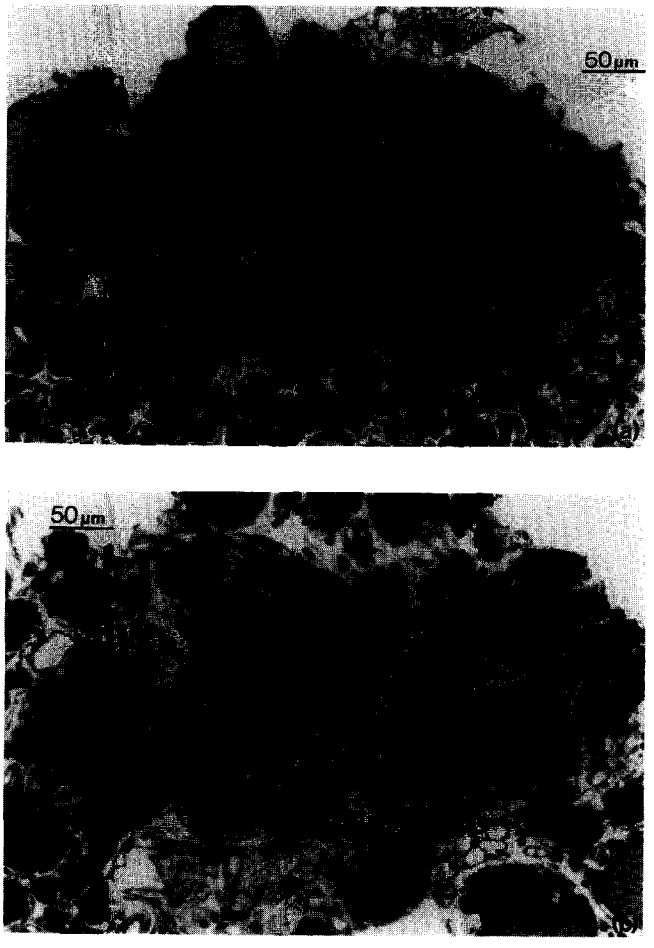

Figure 6. (a) Normal thyroid gland. Haematoxylin and eosin staining, magnification ×200. (b) A focal interstitial oedema with scanty mononuclear infiltration, as well as moderate depletion and flattening of the epithelium of a few follicles in the thyroid as found in a minority of melanoma-bearing mice treated with ^{211}At-MTB, without prior potassium iodide or potassium perchloride blockage of the gland. Haematoxylin and eosin staining, magnification ×200.

DISCUSSION

MTB labelled with a suitable radioisotope, such as ^{211}At, can effectively control the growth and metastatic spread of melanoma, as shown in animal model systems [9, 15–17]. Although in man a probability of melanoma dissemination is strongly correlated with the thickness of the primary tumour [1], once occurring, it constitutes the main obstacle

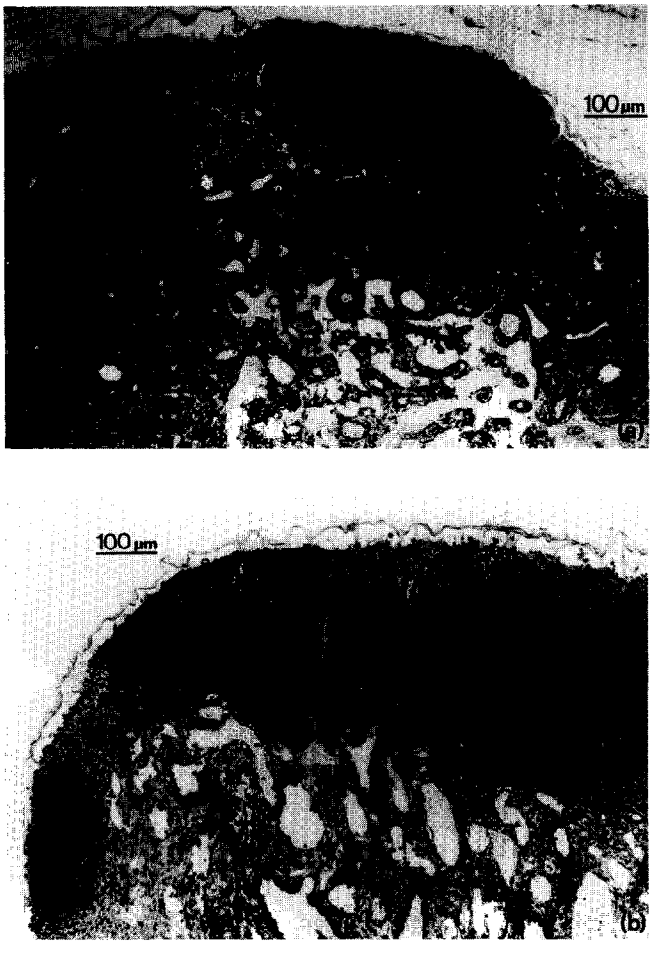

Figure 7. (a) Normal lymph node. Haematoxylin and eosin staining, magnification ×100. (b) A segmental reduction in the number of the cortical small lymphocytes found in a groin lymph node of a mouse bearing pigmented HX118 melanoma and treated with ^{211}At-MTB. Haematoxylin and eosin staining, magnification ×100.

to effective treatment. Thus, the possibility of using ^{211}At-MTB to prevent such a spread by scavenging melanoma cells circulating in blood and eradicating micro-, as well as small macrometastases regardless of their localisation and without the necessity of their prior detection, is of great importance provided the proposed targeted radiotherapy does not lead to severe side-effects. The present results prove that this is the case. Earlier biodistribution studies revealed a rapid clearance of radiolabelled MTB from the blood and most normal organs [10, 11, 23]. Only the liver and kidneys were at potential risk of damage from administered ^{211}At-MTB due to MTB excretion through these structures. However, neither of the two organs disclosed pathological alterations at any stage of the treatment or afterwards. Mild changes in the lymph nodes and the thyroid in a minority of the animals injected with ^{211}At-MTB were the only direct effects of the treatment. Those found in the thyroid could be attributed to a small amount of free $^{211}At^-$ present in the second ^{211}At-MTB preparation rather than to the radiolabelled compound itself, since ^{211}At affinity to the organ is almost as strong as that of iodine [24] and, therefore, the prior blockage of the thyroid with potassium iodide or potassium perchloride would prevent such damage to the tissue. A cause for the reduction in small lymphocyte numbers

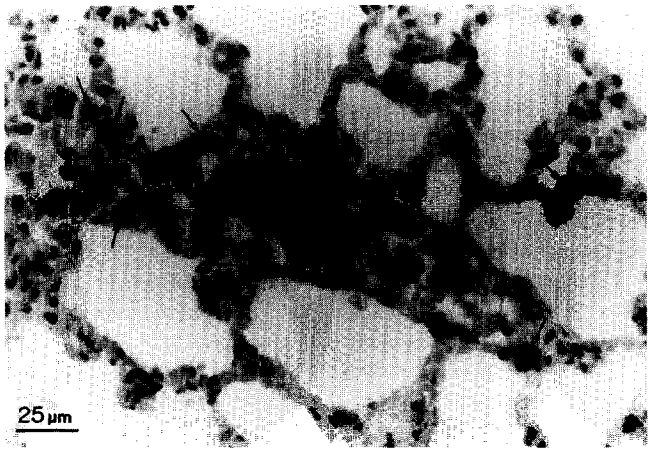

Figure 8. Melanin-laden phagocytic cells (arrows) surrounding a pulmonary blood vessel and present also in the alveolar walls of a mouse bearing HX118 xenografts and treated with ^{211}At-MTB. Haematoxylin and eosin staining, magnification ×400.

by ^{211}At-MTB in the lymph nodes is less obvious. Although both MTB and ^{211}At possess some affinity for the lymphatic tissue [22], this cannot explain ^{211}At-MTB action: the effect was limited to the regional lymph nodes in mice bearing pigmented melanoma only, and observed in a minority of treated animals. Why lymph nodes of animals with pigmented tumours were more vulnerable to ^{211}At-MTB and whether the reduced number of small lymphocytes was a consequence of their damage or induced migration from the organ remain to be answered. However, regardless of the mechanism involved, the pathological changes were temporary and inconsequential for the well-being of the treated mice.

The melanin-laden phagocytic cells found in the lungs not only confirmed the rapidly progressing necrosis of ^{211}At-MTB-treated pigmented tumours but, more importantly, warned against using long-lived radioisotopes for targeted radiotherapy with MTB. Such radioisotopes, attached firmly to melanin via their carrier, would be transferred from the tumours to the lungs and, while deposited there, could cause severe damage.

It is also worth noting that ^{211}At, once bound to its carrier, lost its own characteristic radiotoxicity. A 70-day maximum tolerated dose of 1.5 MBq $^{211}At^-$/mouse reported previously [22] was five times lower than that administered in the form of ^{211}At-MTB as a single injection and 10 times lower than the total ^{211}At-MTB dose applied in our studies.

The negligible ^{211}At-MTB toxicity to normal organs was accompanied by severe damage to the melanoma lesions. The two distinguishable microscopic patterns of tumour response to ^{211}At-MTB treatment observed could not be attributed to the host, as the two tumours grown in the same animal often presented different patterns of damage. Although the immediate response to the treatment always concerned cells surrounding the capillary vessels, the lesions developed differently with time, namely, either to progressive and unresorbed necrosis or by a rapidly declining number of melanoma cells and an abundance of phagocytic cells accumulating primarily in the tumour capsule. Consequently, effectiveness of the treatment as determined macroscopically by measurement of the tumour size was

mirrored faithfully only by the latter lesions. The size of the tumours with unresorbed necrotic tissue grossly underestimated the efficacy of ^{211}At-MTB therapy. It seemed, therefore, that the ability to attract a large number of phagocytic cells by some lesions was responsible for the observed differences in expression of their damage both micro- and macroscopically. This, however, did not influence the overall effectiveness with which ^{211}At-MTB affected the tumours, regardless of their size.

Current results, therefore, re-inforce our previous findings [9, 15–17] concerning the high therapeutic potential of ^{211}At-MTB for pigmented melanomas, and show that ^{211}At-MTB can be successfully applied at the expense of negligible transient damage to normal structures and without impairment of general health [16, 17] (and data presented in this paper). Consequently, the data strongly argue for the introduction of adjuvant therapy with α-particle emitters, such as ^{211}At, provided the radioisotope is bound to a suitable carrier. At the same time, our results revealed serious limitations of the standard method applied to the evaluation of tumour response to the treatment, namely, the macroscopic measurement of tumour size at various time intervals after ^{211}At-MTB administration to animals. Time-dependent changes in the tumour volume did not always faithfully reflect the damage caused by ^{211}At-MTB, often significantly underestimating the therapeutic gain achieved. Thus, such measurements should serve as a preliminary rather than the ultimate criterion in the determination of effectiveness of the applied treatment.

1. MacKie RM, Aitchison T, Sirel JM, McLaren K, Watt DC. Prognostic models for subgroups of melanoma patients from the Scottish Melanoma Group database 1979–86 and their subsequent validation. *Br J Cancer* 1995, **71**, 173–176.
2. Link EM. Targeted radiotherapy of disseminated melanoma with ^{211}At-methylene blue. In Amaldi U, Larsson B, eds. *Hadron Therapy in Oncology*, Excerpta Medica, International Congress Series 1077, Elsevier, 1994, 677–680.
3. Potts AM. The reaction of uveal pigment *in vitro* with polycyclic compounds. *Invest Opthalmol Vis Sci* 1964, **3**, 405–416.
4. Forrest IS, Gutmann F, Keyzer H. In vitro interaction of chlorpromazine and melanin. *Rev Agress* 1966, **VII**, 147–152.
5. Foster R, Hanson P. Electron-donor–acceptor complex formation by compounds of biological interest. I. Optical absorption spectra of mixtures of phenothiazines and related compounds with electron acceptors. *Biochim Biophys Acta* 1966, **112**, 482–489.
6. Foster R, Fyfe CA. Electron-donor–acceptor complex formation by compounds of biological interest. II. The association-constant of various 1,4-dinitrobenzene–phenothiazine drug complexes. *Biochim Biophys Acta* 1966, **112**, 490–495.
7. Larsson B, Tjälve H. Studies on the mechanism of drug binding to melanin. *Biochem Pharmacol* 1979, **28**, 1181–1187.
8. Link EM, Lukiewicz S. A new radioactive drug selectively accumulating in melanoma cells. *Eur J Nucl Med* 1982, 7, 469–473.
9. Link EM, Brown I, Carpenter RN, Mitchell JS. Uptake and therapeutic effectiveness of ^{125}I- and ^{211}At-methylene blue for pigmented melanoma in an animal model system. *Cancer Res* 1989, **49**, 4332–4337.
10. Link EM, Rydzy M. Endoirradiation of neoplastic tissues by administered radioisotopes. In *Proceedings of the Third Meeting of the Polish Biophysics Society*, 1978, 62.
11. Link EM, Costa DC, Lui D, Ell PJ, Blower PJ, Spittle MF. Targeting disseminated melanoma with radiolabelled methylene blue: comparative biodistribution studies in man and animals. *Acta Oncol* 1996, **35**, 331–341.
12. Humm JL. Dosimetric aspects of radiolabelled antibodies for tumour therapy. *J Nucl Med* 1986, **27**, 422–427.
13. Kassis AI, Harris CR, Adelstein SJ, Ruth TJ, Lambrecht R, Wolf AP. The *in vitro* radiobiology of astatine-211 decay. *Radiat Res* 1986, **105**, 27–36.
14. Hall EJ. Linear energy transfer and relative biological effectiveness. In *Radiobiology for the Radiologist*, IVth edn. Philadelphia, Lippincott, 1994, 153–164.
15. Link EM, Carpenter RN. ^{211}At-methylene blue for targeted radiotherapy of human melanoma xenografts: treatment of micrometastases. *Cancer Res* 1990, **50**, 2963–2967.
16. Link EM, Carpenter RN. ^{211}At-methylene blue for targeted radiotherapy of human melanoma xenografts: treatment of cutaneous tumors and lymph node metastases. *Cancer Res* 1992, **52**, 4385–4390.
17. Link EM, Carpenter RN, Hansen G. ^{211}At-methylene blue for targeted radiotherapy of human melanoma xenografts: dose fractionation in the treatment of cutaneous tumours. *Eur J Cancer* 1996, **32A**, 1240–1247.
18. Thomas JM. A lung colony clonogenic cell assay from human malignant melanoma in immune-suppressed mice and its use to determine chemosensitivity, radiosensitivity and the relationship between tumour size and response to therapy. *Br J Surg* 1979, **66**, 696–700.
19. West CML, Sandhu RR, Stratford IJ. The radiation response of V79 and human tumour multicellular spheroids—cell survival and growth delay studies. *Br J Cancer* 1984, **50**, 143–151.
20. Rösch F, Henniger J, Beyer G-J, Dreyer R. Optimization of bombardment conditions of the ^{209}Bi(α,2n) cyclotron production of ^{211}At. *J Radioanal Nucl Chem Lett* 1985, **96**, 319–332.
21. Baker FJ, Silverton RE, eds. *Introduction to Medical Laboratory Technology*. Butterworth Scientific, London, 1976, 299–426.
22. Cobb LM, Harrison A, Butler SA. Toxicology of astatine-211 in the mouse. *Hum Toxicol* 1988, 7, 529–534.
23. Dubois D, Ledermann JA, Link EM, Stauss H, Collins M. Malignant melanoma. *Lancet* 1992, **340**, 948–951.
24. Shaffer RN. Alpha radiation. Effect of astatine-211 on the anterior segment and on an epithelial cyst. *Trans Am Ophthalmol Soc* 1952, **50**, 607–627.

Acknowledgements—The financial support from the Cancer Research Campaign is gratefully acknowledged. We are indebted to Miss Helen Petterson and Mr Paul Tipping of the Photography and Illustration Centre, Middlesex Hospital, for their assistance with the microphotography.